

# HMBA OPTICS CORRECTION EXPERIENCE AT ESRF

S. Liuzzo, N. Carmignani, L. R. Carver, L. Farvacque, P. Raimondi, T. Perron, S. White  
 ESRF, Grenoble, France

## Abstract

The ESRF-EBS storage ring, successfully commissioned in 2020, operates the HMBA lattice, first proposed in [1] and then adopted in several recent upgrade programs [2–4]. The successful and timely commissioning of the storage is in large part due to the excellent optics control achieved over that period. Design performance were obtained with lower than predicted correction strengths, localized for the most part in the vicinity of sextupoles. This remarkable behavior is not only the result of the corrective actions taken during the commissioning but also of the extremely accurate conception and alignment of the machine. This report summarizes the steps that lead to the present performances and discusses their stability over time.

## INTRODUCTION

The new European Synchrotron Radiation Facility (ESRF) Storage Ring (SR) is based on the Hybrid Multi Bend Achromat (HMBA) lattice cell. Relevant parameters and details can be found in [1, 5, 6]. The SR commissioning started in December 2019, and lasted for about three months. The commissioning activities are detailed in [5]. The present document reports on the tuning of optics during commissioning starting from orbit steering and optics correction and finally with the installation of Short Bending (SB) magnets and 2-Pole Wiggler (2PW) sources as described in [7].

## CLOSED ORBIT STEERING

The initial closed orbit featured large distortion of several 100  $\mu\text{m}$  in large part due to uncorrected offsets, a significant static injection bump ( $\sim 6$  mm at injection) and perturbations driven by the necessity to avoid yet to be found obstacles [6]. This large initial value was gradually corrected down to approximately 50  $\mu\text{m}$  rms in both planes. The progress of the corrections can be see in Table 1 together with several relevant parameters. Following, the measurement and correction of BPM offsets using beam based alignment [8] the orbit correction was performed using standard Singular Value Decomposition (SVD) methods as presented in [9]. Simulation based on alignment tolerances predicted that a maximum of approximately 100 singular-vectors could be used over a total of 288 available. Exceeding this value would result in steerers running out of strength [10]. In reality, the better than expected alignment of the SR ( $\sim 35$   $\mu\text{m}$  rms instead of the expected  $\sim 60$   $\mu\text{m}$  rms, see [5]) allowed to operate the machine with correctors strengths well within limits and explore the potential of increasing the number of singular-vectors to better correct the closed orbit. Simulations were used to determine the optimum number of singular-vectors. A set of lattices with random quadrupole

errors ( $\sqrt{\langle \Delta x^2 \rangle} = 60$   $\mu\text{m}$ ,  $\sqrt{\langle \Delta y^2 \rangle} = 40$   $\mu\text{m}$  rms, representing in the simulations orbit rms as the measured ones) was generated and closed orbit correction were performed with increasing number of singular-vectors. Figure 1 shows the results of these simulations. Correcting with 162 singular-vectors in both planes showed a net improvement in dynamic aperture (not shown) and Twiss functions modulation.

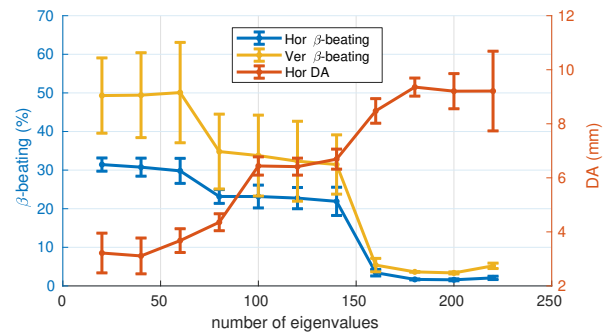


Figure 1: Simulated evolution of beta-beating as a functions of the number of singular vectors used for closed orbit steering in lattices with quadrupole alignment errors of  $\sqrt{\langle \Delta x^2 \rangle} = 60$   $\mu\text{m}$ ,  $\sqrt{\langle \Delta y^2 \rangle} = 40$   $\mu\text{m}$ .

These values were then used in operation and resulted in improved closed orbit with steerers strengths well within limits. By increasing the number of singular-vectors and improving our capabilities to fit localized dipole errors it was possible to detect a missing bending angle in the Dipole-Quadrupole (DQ) magnets. The decomposition in singular vectors of the horizontal steerers pattern present in the SR was showing two interesting features as seen in Fig. 2.

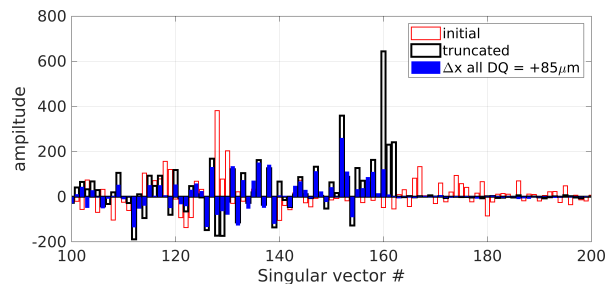


Figure 2: Horizontal steerers decomposition.

First, singular-vectors above 162, where the cut for the correction was placed, were observed, most probably the result of several steerers calibration issues and static injection bump set for injection on-axis. Second, a very strong 162<sup>nd</sup> singular value. The first observation was solved by the truncation of all unwanted singular values, above 162 as seen on the black curve. The second observation moti-

vated a more detailed study of singular vector 162, that was found compatible with the response of DQ magnets alone, indicating a missing angle or misalignment in these magnets. With a systematic correction applied to all DQs, the rms horizontal steerers strength was reduced from 87  $\mu\text{rad}$  to 50  $\mu\text{rad}$  while maintaining and rms closed orbit of 60  $\mu\text{m}$  rms in both planes. Following these observations it was decided to move all DQ1 and DQ2 horizontally by 85  $\mu\text{m}$ , value obtained from the fit of steerers strengths in DQ1 and DQ2 to cancel the singular value 162. These movements allowed to reduce the correction applied on the DQs by a factor 2 showing a positive but yet insufficient displacement. It was later discovered that DQ2 magnets suffered an alignment reference issue that lead to an error of 121  $\mu\text{m}$  [11]. This observation comforted the necessity for this intervention which final results is seen on the blue bars in Fig. 2 for which the vector 162 is strongly reduced.

### Linear Optics Corrections

Linear optics measurements and correction were performed very early and regularly during the commissioning. The first observation of strong optics distortion were estimated from first turn trajectory data that gave a vertical tune error of  $\Delta Q_v = \sim -1.4$  units from the expected model value ( $Q_{v,meas} = 25.9 \pm 0.3$ ,  $Q_{v,theo} = 27.34$ ). The source of this error appeared to be distributed around the ring. This was later confirmed by optics measurements based on Orbit Response Matrix (ORM) acquisition from which an rms  $\beta$ -beating above 20% and an rms dispersion mismatch above 4 mm was derived as seen on the blue curves in Fig. 3 (exact values in Table 1, row 2).

Such large optics errors were not expected and the resulting corrections to fit the measurements were found to be unrealistic. These observations lead to a complete re-assessment of the magnetic model of the lattice that shed light on two major issues. First, due to the compactness of the lattice in the longitudinal direction, significant cross-talks between adjacent magnets exist that alter its magnetic layout. The cross-talks were computed in simulations and then validated by magnetic measurements using the stretched wire method as described in [12]. The predicted impact of these gradient errors on the vertical tune corresponds to a deviation of  $\Delta Q_v = -1.3$  that is comparable to the measured initial value of  $\Delta Q_v \sim -1.4$ . The cross-talks were accounted for by inserting thin elements where appropriate and re-matching the lattice model to the design optics functions. Second, calibration factors were wrongly assigned or suffered from measurements errors resulting in erroneous current to field conversion. The calibration errors found were: wrongly assigned scale factor or magnet serial number, control issues or inexact magnetic measurements (different between ESRF and factory measurements) that accumulated to errors as large as 1%. Optics measurements performed after the cross-talks were integrated in the model and the calibration factors were properly assigned and applied are shown on the red curve (without any quadrupole corrections) in Fig. 3 (yellow curves) and Table 1 row 4. A clear improvement

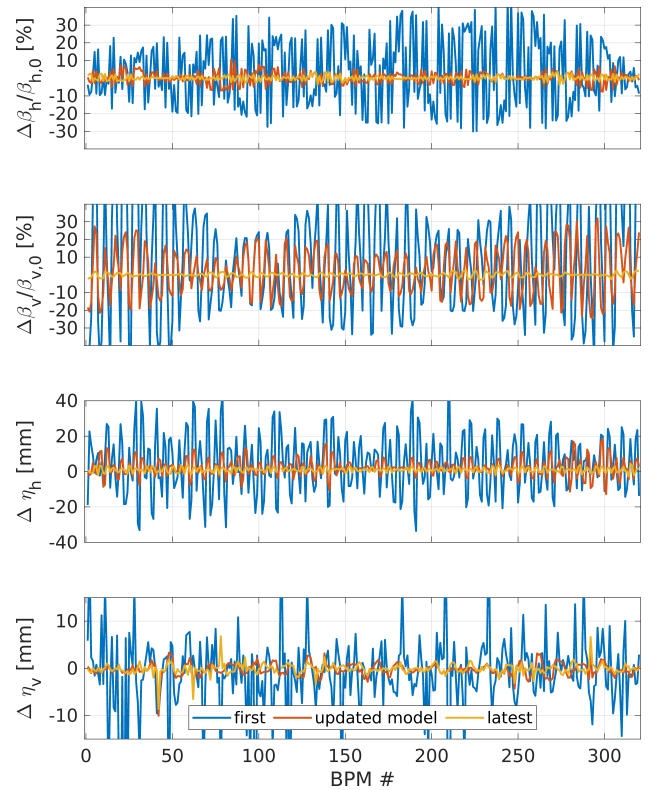


Figure 3: EBS dispersion deviation and  $\beta$ -beating. (blue) First measured; (red) after introduction of cross talks, calibration, BBA, steering, no optics correction; (yellow) after optics correction.

with respect to the initial situation is observed. These conditions represent the machine that we ought to find if we had started with modeled cross-talks and correct calibrations. With these large errors removed accurate optics corrections were made possible. Hysteresis of the steerers used for ORM measurement [9] and large steerers scale factors add to be taken in account for appropriate measurements. The final results are shown in Fig. 3 (and in Table 1 row 7). The present situation, is the result of several iterations that converged to  $\Delta\beta/\beta_h \approx 1.5\%$  and  $\Delta\beta/\beta_v \approx 1.5\%$ ,  $\Delta\eta_h \approx 2.0$  mm and  $\Delta\eta_v \approx 1.0$  mm. Injection efficiency  $I.E.TL2-SR > 80\%$  is routinely achieved in these conditions (off-axis parallel bump, gaps open). A remarkable feature of the HMBA lattice is that lattice corrections are applied only on quadrupole magnets located in the direct vicinity of sextupoles. This shows that optics errors are for the most part dominated by the feed-down effects in sextupole magnets driven by non-zero closed orbit at their location, as expected from the model. This confirms that the construction, magnetic measurements and modeling of the lattice magnets is very accurate and that no strong calibration or unexpected localized errors are left in the machine. Furthermore, the corrections strengths required were decreasing as far as optics corrections and model improvements progressed, proving a better understanding of the lattice. Coupling and vertical dispersion corrections were performed and applied in parallel

Table 1: Optics parameter and correction strengths evolution for peculiar moments during the EBS commissioning, undulators gaps open. 1) start of commissioning, off axis injection, first tune estimate; 2) SVD-truncation, first RM; 3) first accumulation; 4) cross talks, calibrations, BBA, quadrupole corrections to zero; 5) DQ realignment +85um, BBA; 6) installation of BM 29 30; 7) present status, pinholes adjustment.

date	$\epsilon_h$	$\epsilon_v$	x	y	$\Delta\eta_h$	$\Delta\eta_v$	$\Delta\beta_h$	$\Delta\beta_v$	$\Delta\theta_h$	$\Delta KL_q$	inj.eff.	$\tau$	$I_{max}$
units	pm	pm	$\mu\text{m}$	$\mu\text{m}$	mm	mm	%	%	$\mu\text{rad}$	$10^{-4}/m$	%	h	mA
error	$\pm 19$	$\pm 1$	$\pm 1$	$\pm 1$	$\pm 0.1$	$\pm 0.1$	$\pm 1$	$\pm 1$	$\pm 0.1$	$\pm 10^{-5}$	$\pm 3$	$\pm 0.1$	$\pm 0.01$
	gaps open										*=off-axis		
1) 2019 11 28			2976.7	1122.7					0.0	0.0			0.0
2) 2019 12 12	676.7	80.9	328.3	158.5	23.6	4.3	19.5	34.0	62.1	0.0			0.2
3) 2019 12 17	215.0	10.0	229.5	145.3					52.1	31.3	0.2		6.4
4) 2020 01 23	195.6	12.5	98.8	110.6	5.1	1.3	3.4	13.3	65.1	13.6	5.0		2.5
5) 2020 02 21	164.9	5.0	89.6	62.0	2.1	1.1	1.6	1.3	47.3	29.7	93.0		160.0
6) 2020 03 10	157.0	0.6	42.9	55.8	2.5	1.2	0.5	0.5	65.1	17.4	88.0*		201.0
7) 2020 12 13	140.8	0.5	53.2	52.8	1.9	1.2	1.6	1.1	62.1	16.1	>80.0*	22.0	201.0

to linear optics corrections using the same ORM measurements. All available (288) skew quadrupoles were used for these corrections. Measured vertical emittance of  $\epsilon_v = 1 \pm 1$  pm is systematically obtained after coupling corrections without any further tuning, however this value should be taken with great care as it is at the limit of the resolution of the pinhole cameras. In User Service Mode operation, the vertical emittance is stabilized at 10 pm using a feedback loop injecting white noise in the vertical plane. Tune and chromaticity working point scans were performed routinely and confirmed the simulations [13, 14] with an operation tune working point close to the predicted (.21, .34) and large chromaticities being beneficial in terms of Touschek lifetime. The present working values are  $Q_{(h,v)} = (.18, .34)$ ,  $\xi_{(h,v)} = (9.2, 7.9)$

### Integration of Bending Magnet Beamlines

The initial commissioning of the HMBA lattice was performed without the bending magnet (BM) sources installed to facilitate the optics commissioning. 16 such beamlines were then installed gradually during the beamlines commissioning period [15]. The installation of 2PW and SB require to adjust the alignment of magnets around the source to compensate for its impact on lattice geometry and dispersion as shown in [7].

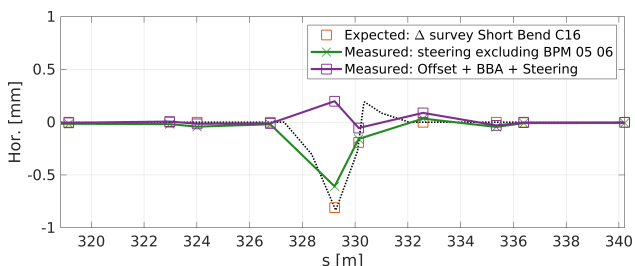


Figure 4: SB installation. Close to expected BPM reading are obtained after installation of SB in cell 16. The corresponding BPM offsets are set and remeasured for final orbit steering.

As a first test one 2PW and 1 SB were installed simultaneously and the optics correction predicted from theory applied (small compared to already applied optics corrections). Following this intervention no first-turns steering was necessary as stored beam and accumulation were immediately possible without any correction. Row 6 in Table 1 lists the parameters of the lattice after installation of 1 SB and 1 2PW. Similar results were achieved for each BM source installation, including up to six BM sources simultaneously. For the specific case of the SB, further validation of the successful realignment is given by closed orbit measurements. Providing the movements were applied to magnets only, large BPM to quadrupoles offsets were expected. This is shown in Fig. 4 where the expected and measured closed orbits are shown. BBA measurements showed a variation of BPM offset values within 50  $\mu\text{m}$  from the expected ones.

## CONCLUSION

The EBS SR optics are presently corrected to the expected levels and allowed to improve the modelling of the SR. The major sources of optics distortion (Dipole Quadrupole alignment, cross-talks fields and calibration errors) were taken in account in the model with improvements in terms of final optics parameters and reduced required correction strengths. The EBS lattice features excellent orbit and optics stability thanks to the engineering choices and to the limited sextupole correction used. Simple orbit and tune corrections are sufficient to restore the state of the machine optics even after long shut down periods. Recently small drifts in the tuning have been observed. Few hours of non-linear magnets optimizations usually recover the working conditions within few hours of dedicated machine time.

## REFERENCES

[1] J. C. Biasci *et al.*, "A low-emittance lattice for the ESRF", in *Synchrotron Radiat. News*, vol. 27, no. 6, pp. 8-12, 2014. doi:10.1080/08940886.2014.970931

- [2] T. E. Fornek, “Advanced photon source upgrade project preliminary design report”, ANL, IL, USA, Rep. APSU-2.01-RPT-002, Sep. 2017.
- [3] C. G. Schroer *et al.*, “Petra IV: the ultralow-emittance source project at DESY”, *J. Synchrotron Radiat.*, vol. 25, no. 5, pp. 1277–1290, Sep. 2018.  
doi:10.1107/S1600577518008858
- [4] H. Tanaka, “Current status of the SPring-8 upgrade project”, *Synchrotron Radiat. News*, vol. 27, no. 6, pp. 23–26, Nov. 2014. doi:10.1080/08940886.2014.970935
- [5] P. Raimondi *et al.*, “EBS optics commissioning”, in preparation.
- [6] S. White *et al.*, “Commissioning and restart of ESRF-EBS”, presented at the 12th Int. Particle Accelerator Conf. (IPAC’21), Campinas, Brazil, May 2021, paper MOXA01, this conference.
- [7] S. Liuzzo *et al.*, “Optics Adaptations for Bending Magnet Beam Lines at ESRF: Short Bend, 2-Pole Wiggler, 3-Pole Wiggler”, in *Proc. 8th Int. Particle Accelerator Conf. (IPAC’17)*, Copenhagen, Denmark, May 2017, pp. 666–669. doi:10.18429/JACoW-IPAC2017-MOPIK062
- [8] A. Wolski and F. Zimmermann, “Closed orbit response to quadrupole strength variation”, LBNL, Berkeley, USA, Rep. LBNL-54360, Jan. 2004.
- [9] Y. Chung, *et al.*, “Closed orbit correction using singular value decomposition of the response matrix”, in *Proc. 15th Particle Accelerator Conf. (PAC’93)*, Washington D.C., USA, Mar. 1993, pp. 2263–2266. doi:10.1109/PAC.1993.309289
- [10] S. Liuzzo, “Corrections strengths are limited by PS”, internal ESRF presentation, Feb. 2018.
- [11] Private communication.
- [12] G. Le Bec *et al.*, “Cross-talks between storage ring magnets at the Extremely Brilliant Source”, submitted for publication.
- [13] S. Liuzzo *et al.*, “Updates on Lattice Modeling and Tuning for the ESRF-EBS Lattice”, in *Proc. 7th Int. Particle Accelerator Conf. (IPAC’16)*, Busan, Korea, May 2016, pp. 2818–2821. doi:10.18429/JACoW-IPAC2016-WEPOW005
- [14] N. Carmignani *et al.*, “Linear and Nonlinear Optimizations for the ESRF Upgrade Lattice”, in *Proc. 6th Int. Particle Accelerator Conf. (IPAC’15)*, Richmond, VA, USA, May 2015, pp. 1422–1425. doi:10.18429/JACoW-IPAC2015-TUPWA013
- [15] S. Liuzzo *et al.*, “ESRF-EBS lattice model with canted beam-lines”, *J. Phys. Conf. Ser.*, vol. 1067, p. 032006, Sep. 2018. doi:10.1088/1742-6596/1067/3/032006